BAOJ Cancer Research & Therapy

Pulimamidi Rabindra Reddy, et al., BAOJ Cancer Res Ther 2017 3: 2
3: 036

Research

N-(4-Amino-1,2,5-Oxadiazole-3-YL) Picolinamide Cu(II) Complexes for Anti-Cancer Activity

Pulimamidi Rabindra Reddy[1]*, Ravula Chandrashekar[1], Battu Satyanarayana[1] and Madamsetty Vijay Sagar[2]

[1]*Department of Chemistry, Osmania University, India*

[2]*Biomaterials Group, CSIR-Indian Institute of Chemical Technology, India*

Abstract

Two new Cu(II) complexes binary [Cu(II)(DFPA)Cl] (1:1) (1) and ternary [Cu(II)(DFPA)(8HQ)](1:1:1) (2), where DFPA is N-(4-Amino-1,2,50-Oxadiazole-3-yl) Picolinamide derived from the amide linkage of picolinic acid and 3,4-diaminofurazan with HATU reagent, were synthesized and characterized. Complexes 1 and 2 exhibit square planar and square pyramidal geometries respectively where DFPA acts as a tridentate N,N,N donor ligand and 8HQ acts as N,O donor ligand. The interactions of the complexes with calf thymus DNA (CT-DNA) were investigated using UV-Vis, fluorescence and Circular Dichroism (CD) spectral studies. CT-DNA binding studies revealed that the complexes bind through an intercalative mode and show good binding propensity (Intrinsic binding constant K_b: $1.1x10^4$ M^{-1} (1), $1.32x10^4$ M^{-1} (2), Stern-Volmer Quenching constant K_{sq}: 0.95 (1), 1.47 (2)). The docking data reveal that the complexes 1 and 2 bind to DNA through an intercalative interaction, a preferred mode of interaction for anti-cancer activities. The DNA cleavage activity of complexes 1 and 2 were also studied using gel electrophoresis. The cleavage takes place through hydrolytic path way. In addition, *in vitro* cytotoxicity of the complexes and DFPA ligand towards HeLa, MiaPaca-2, B16F10, for cell viability were assayed by the MTT method. The cytotoxicity of complex 1 is comparable with that of Cis-Platin, where as complex 2 exhibits much higher cytotoxicity than Cis-Platin suggesting a promising future drug. Cellular uptake properties on HeLa cell line was studied by confocal microscopy.

Key Words: Cu(II) complexes; Calf thymus DNA; DNA binding-Cleavage; Fluorescence spectra Docking; Anti-Cancer Activity

Introduction

DNA is the intracellular target in treating a wide range of diseases; the interaction of co-ordination compounds with DNA has been of interest due to their possible applications in cancer therapy [1-5]. The interaction of metal ions with drugs administrated to therapeutic purposes is a subject of considerable interest. It is known that some drugs work by chelation or inhibiting the formation of metal enzymes [6,7], therefore metal ions might play a vital role during the biological process of drug utilization in the body [8,9]. In recent years, the interest in this field has shifted to non-platinum based agents in order to find better cytotoxicity with lesser side effects. Cu(II) based complexes appear to be an attractive and promising candidate for anticancer therapy [10].

The ability of Cu(II) complexes to bind to DNA and exhibit nuclease activity in the presence of reducing agents is well established. The type of organic ligands in such copper complexes seems to affect and regulate their activity. They (a) neutralize the electric charge of the copper ion, (b) increase the lipophilicity of the complex facilitating transport through cell membrane, and (c) intercalate to DNA or interact non covalently with proteins. The biological activity of the ligand is usually increases upon complex formation, due to its ability to create required interactions with DNA, the target molecule. Our ligand analogs are already part of the analgesic drugs. Therefore, the complex2 has great potential to be prospective drugs. 1,2,5-Oxadiazazole is a heterocyclic compound containing an oxygen and a nitrogen atoms in five-membered ring. It is derived from furan by substitution of two methylene groups with two pyridine type nitrogenes. Oxadiazoles are more widely studied by researchers because of their important chemical, physical and biological properties. Furoxan and benzofuroxan analogs were recently found to be potent anticancer, antimicrobial,

***Corresponding author:** Pulimamidi Rabindra Reddy, Department of-Chemistry, Osmania University, Hyderabad – 500 007, India, fax: +91-40-27090020; phone: +91-40-27171664, e-mail: profprreddy@gmail.com

Sub Date: March 30, 2017, **Acc Date:** May 30, 2017, **Pub Date:** June 1, 2017.

Citation: Pulimamidi Rabindra Reddy, Ravula Chandrashekar, Battu Satyanarayana and Madamsetty Vijay Sagar (2017) N-(4-Amino-1,2,5-Oxadiazole-3-YL) Picolinamide Cu(II) Complexes for Anti-Cancer Activity. BAOJ Cancer Res Ther 3: 036.

anti aggregating, antiulcer, and immunosuppressive agents. Similarly, biological studies revealed that oxadiazolopyrazines, furazans, and diaminofurazans exhibited significant antibacterial properties and also showed the active use in the treatment of cancer, atherosclerosis, angiogenesis, neurodegenerative diseases, and inflammatory diseases [11-23]. Picolinic acid is a six- member ring structure compound that has been detected in a variety of biological mediums including, cell culture supernatants, blood serum [24], human milk, pancreatic juice and intestinal homo genates [25-27]. It was shown that treatment with picolinic acid disordered the cell growth and arrested cell cycle [28]. Picolinic acid also stimulates programmed cell-death [PCD] in cancer cells and efficiently interrupts the progress of HIV in vitro. 8-Hydroxy quinoline (8HQ) and some of its derivatives exhibit substantial cytotoxic activity against cancer cells [29]. Since the 8-hydroxyl–quinole has good chelating ability to the metal ions, recently a series of transition metal complexes with 8-hydroxy quinoline derivatives having good anti cancer ability have been reported [30]. Herein, we describe the synthesis, spectroscopic characterization of two new Cu(II) complexes [Cu(II)(DFPA)Cl] (1:1) (1), [Cu(II)(DFPA)(8HQ)](1:1:1) (2) (Scheme 1). *In vitro* DNA binding profile of complexes 1 and 2 with CT-DNA was carried out by employing UV-Vis, fluorescence spectra and Circular Dichroism (CD) spectral studies. Complexes 1 and 2 exhibits chemical nuclease activity cleaving PUC 19 plasmid DNA via hydrolytic pathway. Furthermore, the cytotoxicity of the complexes against the HeLa, MiaPaca-2 and B16F10 cell line was surveyed by the MTT assay. Cellular uptake properties on HeLa cell line was studied by confocal microscopy.

Experimental Section

Materials and Instruments

General 3,4-Diaminofurazan, picolinic acid, HATU, ethidium bromide (EB), $CuCl_2.2H_2O$ and $Cu(OAC)_2.4H_2O$ (99.99% purity), were obtained from Sigma, USA. All other chemicals and solvents (spectroscopic grade) were purchased from commercial sources and were used without further purification. Doubly distilled water was employed for the preparation of the buffer solutions. Calf thymus (CT) DNA was obtained from Fluka (Switzerland). Supercoiled (SC) plasmid pUC19 DNA and Tris-HCl buffer were obtained from Bangalore Genei (India). The spectroscopic titrations were carried out in aerated buffer (5 mM Tris HCl/ 50 mM NaCl, pH 7.5) at room temperature. Elemental analysis data were obtained from the micro analytical Heraeus Carlo Erba 1108 elemental analyzer. ESI mass spectra of 1 and 2 were recorded using a quattro Lc (Micro mass, Manchester, UK) triple quadrupole mass spectrometer with Mass Lynx software. The molar conductivity was measured on a Digisun Digital conductivity bridge (model: DI-909) with a dip

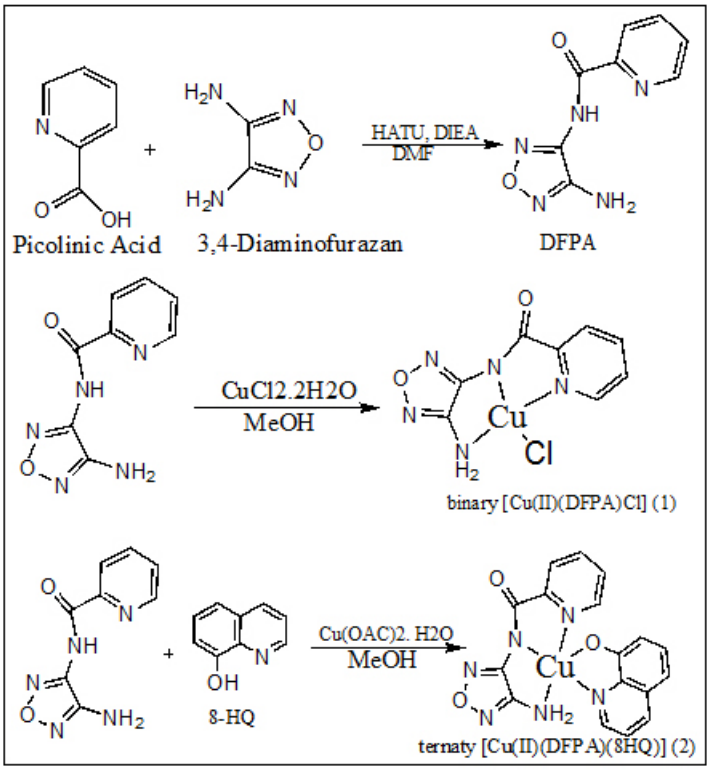

Scheme 1. Syntheses of complexes **1** and **2**.

typecell. Infrared spectra were recorded on a Shimadzu -1600 IR spectrometer, in KBr pellets in the 4000-400 cm^{-1} range. UV-Vis spectra of the complexes were recorded on Shimadzu (160A) UV-Visible spectrophotometer using 1-cm quartz micro-cuvettes (800-200nm). Magnetic susceptibilities of the complexes were recorded at room temperature on a Faraday balance (CAHN-7600) using $Hg[Co(NCS)_4]$ as the standard. Diamagnetic corrections were made by using Pascal's constants [31]. X BAND EPR Spectra of complexes were recorded at room temperature on JEOL-FA200 ESR spectrometer at university of Hyderabad.

Synthesis

Synthesis of Ligand (DFPA): For the synthesis of DFPA ligand, 2-picolinic acid (0.5 g, 4.06 mmol) was dissolved in dry DMF (15 ml) and HATU (1.47g, 6.07 mmol) and DIEA (1.04g, 8.04 mmol) were added. The solution was cooled to 0˚C. It was stirred for 30 min followed by the addition of 3,4-diamino furazan (0.40g, 4.05 mmol). The mixture was warmed to room temperature and the stirring was continued for another 12 h. After the workup, the solvent was removed under reduced pressure. It was then purified by column chromatography on silica gel.

Synthesis of Binary Complex [Cu(II)(DFPA)Cl] (1): A solution of DFPA (1.00 g, 4.87 mM) in methanol (8 ml) was added to an aq. methanolic solution (10 ml) of $Cu(OAC)_2.4H_2O$ (0.71 g, 3.58 mM).The mixture was stirred for 8 h at room temperature; dark green precipitate (complex 1) was separated from the solution by suction filtration, purified by washing several times with methanol and dried for 24 h under vacuum.

Synthesis of Ternary Complex [Cu(II)(DFPA)(8HQ)] (2): A solution of DFPA (1.00g, 4.87 mM) in methanol (8 ml) was added to an aq. methanolic solution (10 ml) of $CuCl_2.2H_2O$ (0.83 g, 4.89 mM). The mixture was stirred for 8 h at room temperature. The heterocyclic base [8HQ] (0.77 g, 5.3mM) dissolved in methanol (6 ml) was added drop wise to a methanolic solution mixture. The light green precipitate (complex 2) was stirred for 6 h. After completion of reaction (confirmed by TLC), precipitate was separated from the solution by suction filtration, purified by washing several times with methanol and dried for 24 h under vacuum.

Analytical Data

DFPA: (Yield: 90%).M.P: 140-145°C.IR: ν_{max} / cm^{-1}: 3429s, 3329s, 1620s, 1568m, 1458m, 1352m . ^1H NMR (300MHz, $CDCl_3$) δ 10.82 (s, 1H); 8.85 (d, 1H); 8.43 (d, 1H); 7.93 (m, 1H); 7.64 (m, 1H); 5.381 (bs, 2H); . ESI-MS: m/z 205 $[M^+]$. ^{13}C NMR (75MHz, $CDCl_3$): δ 163.2, 151.1, 148.5, 147.3, 137.9, 127.6, 122.9.

[Cu(II)(DFPA)Cl] (1): (Yield: 75%). M.P: 280°C. UV-Vis in MeOH: λ_{max}/nm: 211, 258, 655. IR: ν_{max} / cm^{-1}: 3387s, 3315s, 2312s,1658s, 1593s , 1454s, 1371s, 1267s, 1029s, 844s, 798s, 759s, 684s, 559s (Cu-N), 422m(Cu-O), 293 (Cu-Cl). ESI-MS in MeOH: *m*/*z* 301 $[M^+-2H]^+$. Elemental analyses: Calc. for $C_8H_6ClN_5O_2Cu$: C, 31.69; H, 1.99; N, 23.10; Cu, 20.96 %. Found: C, 30.96; H, 1.89; N, 23.34; Cu, 19.82 %. μ_{eff} = 1.80 BM. Λ_M [$\Omega^{-1}Cm^2\,M^{-1}$, 10^{-3} M aq. methanol solution, 25°C]:12.

[Cu(II)(DFPA)(8HQ)] (2): (Yield: 80%). M.P: 270-295°C. UV-Vis in MeOH: λ_{max}/nm: 227, 254, 276, 649. IR: ν_{max} / cm^{-1}: 3383w, 3045w, 2978s, 1573s, 1496s, 1321m, 1276s, 1111s, 823s, 736s, 522s(Cu-N), 405s(Cu-O), 289s(Cu-Cl). ESI-MS in MeOH: *m*/*z* 411 $[M^+]$. Elemental analyses: Calc. for $C_{17}H_{12}N_6O_3Cu$: C, 49.58; H, 2.94; N, 20.40; Cu, 15.43 %. Found: C, 50.12; H, 2.89; N, 20.51; Cu, 15.55%. μ_{eff} = 1.80 BM. Λ_M [$\Omega^{-1}Cm^2\,M^{-1}$, 10^{-3} M aq. methanol solution, 25°C]:10.

DNA Binding

Preparation of Stock Solutions: Concentrated CT-DNA stock solution was prepared in 5mM Tris-HCl/50mM NaCl in water at pH=7.5 and the concentration of DNA solution was determined by UV absorbance at 260 nm. The molar absorption coefficient was taken as 6600 $M^{-1}cm^{-1}$ [32]. Solution of CT-DNA in 5 mM Tris-HCl/50 mM NaCl gave a ratio of UV absorption at 260 nm and 280 nm A_{260}/A_{280} of ca. 1.8-1.9, indicating that the DNA was sufficiently free of protein [33]. All stock solutions were stored at 4 °C and were used within four days. The concentration of EB was determined spectrophotometrically at 480 nm (e = 5680 $M^{-1}cm^{-1}$) [34]. The DNA binding experiments were done in Tris HCl buffer (5mM Tris-HCl/50mM NaCl) (pH =7.5) using 1 mM MeOH solution of complexes (1 and 2).

Absorption Spectra

Absorption spectra were recorded on SHIMADZU 160A UV-Visible spectrophotometer using 1-cm quartz micro-cuvettes. Absorption titrations were performed by keeping the concentration of the complexes constant (10μM), and by varying [CT-DNA] from 0-10 μM. In the reference cell, a DNA blank was placed so as to offset any absorbance due to DNA at measured wavelength. For the complexes 1 and 2, the binding constants (K_b), were determined from the spectroscopic titration data using the following equation 1:

$$[DNA]/(e_a-e_f) = [DNA]/(e_b-e_f) + 1/K_b(e_b-e_f) \quad \text{.....(1)}$$

The 'apparent' extinction coefficient (e_a) was obtained by calculating A_{obsd} / [Cu]. The terms e_f and e_b correspond to the extinction coefficients of free (unbound) and the fully bound complexes, respectively. A plot of $[DNA]/(e_a-e_f)$ Versus [DNA] will give a slope $1/(e_b-e_f)$ and an intercept $1/K_b$ (e_b-e_f). K_b is the ratio of the slope and the intercept.

Fluorescence Spectral Studies

Fluorescence spectra were recorded with an *Elico* spectrofluorimeter (model Sl 174) equipped with a 450W Xenon lamp. The slit widths

were 2x2x2x2 and the emission spectral range was 550-650 nm. Fluorescence titrations were carried out in 5 mM Tris-HCl/50 mM NaCl (pH =7.5). Quenching experiments were carried out by successive addition of 0-120 μM of the Cu(II) complexes to the DNA (50 μM) solutions containing 50 μM EB. The solutions were excited at 540 nm and fluorescence emission, which corresponds to 598 nm were recorded. The samples were shaken and kept for 2-3 min for equilibrium and then the spectra were recorded.

Circular Dichroism Spectra: A Circular Dichroism (CD) spectrum of CT-DNA was measured in the presence of the increasing concentration complexes 1 and 2 using a J-810 CD spectropolarimeter (JASCO) with a 150 W Xe arc lamp. The instrument was controlled by Spectra Manage software (JASCO). Quartz cells with a path length of 0.5 cm were used and a scanning speed of 100 nm min^{-1} was selected. The data were expressed in terms of mdeg. An appropriate buffer solution running under the same conditions was used as a blank and this result was subtracted from the sample spectra. The CD spectra is an average of three independent scans. Spectra were run between 230 and 330 nm for DNA in the presence of the two complexes 1 and 2.

Docking studies: Patch Dock server [35,36] , was used to perform docking between metal complexes and B-DNA (PDB ID: 423D). For docking studies all the heteroatoms of B-DNA have been deleted including water and polar hydrogen atoms were added. The PDB files of both the DNA and metal complex were uploaded to Patch Dock server. The RMSD (Root mean square deviation) was set at 4 A, the rest of the parameters are being at the default settings. Patch Dock results were obtained as a set of scoring functions based on the shape complementary and the atomic de-solvation energy of the transformed complex.

PDB ID: 432D: DNA (5'-D(*AP*CP*CP*GP*AP*CP*GP*TP*CP *GP*GP*T)-3')

DNA Cleavage

Agar-gel electrophoresis experiments were performed with pUC19 DNA at pH 7.5 in Tris. HCl buffer solution. Hydrolytic DNA cleavage experiment was monitored by the addition of varying concentration of the complexes to 2 μL of pUC19 DNA, the total volume was increased to 16 μL by adding 5 mM Tris HCl/ 5 mM NaCl buffer. After mixing, DNA solutions were incubated at 37°C for 3h. The reactions after incubation were quenched by the addition of 2 ml gel loading dye (0.25% bromophenol blue, 0.25% xylene cyanol, 40% glycerol and 2 mM EDTA). The samples were subjected to electrophoresis for 2h. at 60V on 1% agarose gel in TAE (Tris acetic acid EDTA buffer). The gel was stained with 0.5 mg/ml EB and photographed under UV light. The extent of DNA cleavage was determined by measuring the intensities of the bands using the Alpha Innotech Gel documentation system.

***In Vitro* Cytotoxicity Evaluation by the MTT Assay:** To study the effects of the complexes 1 and 2 on cell growth, HeLa (human breast adenocarcinoma cell line), MiaPia-2 and B16F10 cells growing exponentially were added to 96-well plates (Tarson Ltd) at a density of 3×10^3 per well after counting on Bright Line Haemocytometer (Thermo Scientific). Cells were grown according to the American Type Culture collection (ATCC) instructions. The number of cells were selected to avoid potential over confluence of the cells. Cells were maintained at 37°C and 5% CO_2 in a humidified incubator till cells adhered and reached 70-80% confluency. The cells were treated with the ligand and complexes 1 and 2 (2.5-20μM) at three different concentration for 24 hrs and 0.5% (v/v) DMSO considered as control to ensure an equal volume of 200 μL complete media (RPMI1640+10% FBS) across the plate. The MTT (Tetrazolium bromide salt) compound was used for the measurement of cytotoxicity happen through mitochondrial activity of viable cells by the reduction of Tetrazolium bromide salt and metabolically active cells to form in soluble Formazon crystals which is in yellow colour and solubilized by the addition of detergent. After incubation of 96 well plate with Cu (II) complexes, MTT reagent (Sigma Aldrich) was added to each well working concentration of 0.4Mg/ML prepared in complete medium, and the plate were placed to the incubator for 3 hrs incubation period. After MTT reagent treatment, the medium was discarded, and added 100μ L of DMSO (Cell Culture Grade Sigma Aldrich) plate were agitated gently for 5 mins before measuring the colour was quantified by Bio-Rad Model 680 X ELISA plate readers at optimized absorbance is 570nm. Complexes were dissolved in DMSO and a blank sample containing the same volume of DMSO was taken as the control to identify the activity of the solvent in this experiment. Cisplatin was used as a positive control to assess the cytotoxicity of the tested complexes. This data from cancer cell lines were acquired from triplicate independent cell passages and the IC_{50} values were calculated from the plot of cell viability with different concentration of complexes 1 and 2.

Cells Preparation for Confocal Microscopy: HeLa cells were grown in a phenol red RPMI1640 medium with 10% FBS fetal bovine serum and 1% Pen Strep glutamine (Hi Media) in an atmosphere of 5% (v/v) CO_2-enriched air at 37°C. For microscopic studies, cells were cultured on cover slips (Corning 22X22 mm) incubated till reached 80% confluency for complexes 1 and 2 treatment. Followed by cells were treated with 10μM complexes for 24 hrs, the cells were rinsed with cold PBS (Phosphate Buffer Saline) buffer solution before stained with DAPI (Fluorescent dye). For solvation of dye, dye was diluted with double distilled water. For microscopic studies cells were stained with 50 nM dye and then incubated for about 10 mins. Confocal imaging studies was carried out on one set with DAPI and one set with unstained used as control. Here DAPI was used for nuclear localisation in live cells.

Results and Discussion

Synthesis and Characterization

The ligand (DFPA) was synthesized (Scheme 1) by coupling picolinic acid and 3,4-diaminofurazan with HATU reagent. The DFPA was characterized by ^{1}H NMR (Figure 1), ^{13}C NMR (Figure 2), IR (Figure S1); §ESI), ESI-MS (Figure S3; §ESI). The corresponding Cu(II) complexes (1 and 2) were synthesized (Scheme 1) and characterized by elemental analyses, ESI-MS, IR, UV-Vis, magnetic moment and molar conductance (Table 1). The complexes were highly soluble in DMSO. They were non-hygroscopic and stable both in solid and solution phases. The analytical data are in good agreement with the molecular formulae of the complexes.

ESI-MS Spectra: The ESI-MS studies confirmed the formula proposed for the complexes 1 and 2. ESI-MS of 1 recorded in positive mode gave a peak at *m/z* 301, indicating the presence of complex 1 as $[M\text{-}2H]^{+}$. Complex 2 gave a peak at *m/z* 411, suggesting the presence of complex as $[M]^{+}$ (Figure S3 (a&b); §ESI).

Infrared Spectra: The FT-IR spectral data of the free ligand DFPA and the Cu(II) complexes with their relative assignments have been studied to characterize their structures. The assignments of the IR spectra were made on the basis of literature and Nakamoto [37]. The IR spectra of the complexes were analyzed in comparison with their free ligand spectra. The IR spectra of DFPA ligand exhibited a sharp peak at 3429 cm^{-1} which was attributed to the υ(N-H) vibrations, which disappeared in the complexes due to the deprotanation of amide group upon complexation with copper. This indicates that the nitrogen atoms of the amide group coordinated to Cu(II) ion. An intense stretching absorption band at 1620 cm^{-1} due to the amide carbonyl group υ(C=O) of DFPA, shifted to 1593, and 1573 cm^{-1} in 1 and 2 resp. The peaks corresponding to the ring stretching frequencies ν(C=C) and ν(C=N)) at 1568, 1458 cm^{-1} were shifted to lower frequencies upon complexation, indicating the coordination of the heterocyclic nitrogen atoms to the metal ion. The other non-ligand peaks at 559 and 522$cm^{-1}$for 1 and 2 resp. were assigned to υ(Cu-N) vibration, which is also indicating that the ligands are coordinated to copper through nitrogen atoms. The IR spectral details are given in supplementary information (Figure S2 (a&b); §ESI).

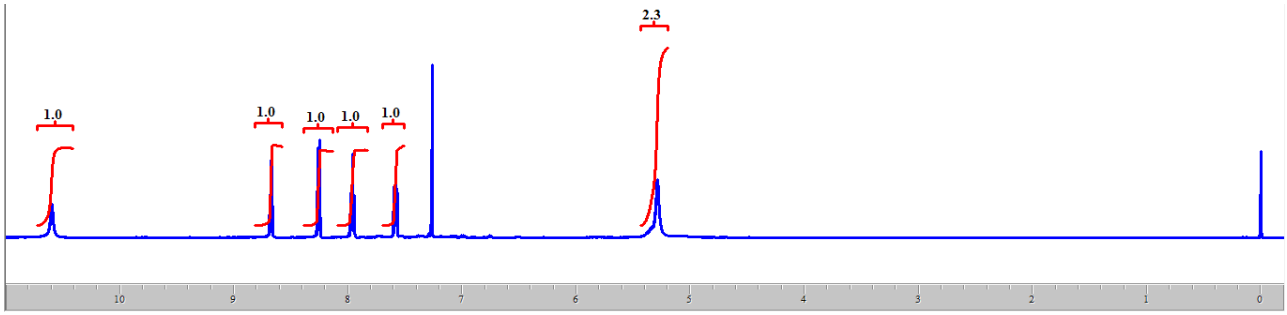

Fig. 1. ^{1}H-NMR spectrum of DFPA ligand.

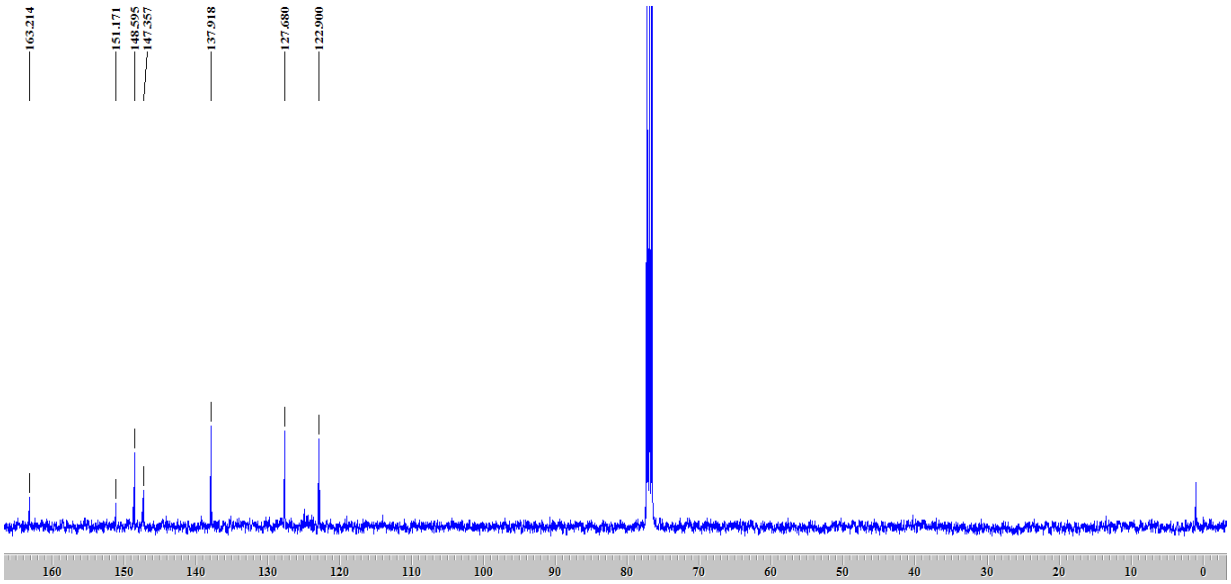

Fig. 2. ^{13}C-NMR spectrum of DFPA ligand.

Table 1. Physicochemical and DNA binding data of complexes **1** and **2**.

	ν(Cu-N) / ν(Cu-O)/[[a]	UV-Vis[b]	ESI-MS	Λ_M [c]	μ_{eff} [d]	K_b [e]	K_{sq} [f]
[Cu(II)(DFPA)Cl] (**1**)	559 422	211, 258, 627	301	10	1.80	$1.1x10^4$	0.95
[Cu(II)(DFPA)(8HQ)] (**2**)	522 405	227, 254, 649	411	12	1.80	$1.32x10^4$	1.47

[a] IR (KBr phase, cm^{-1}); [b] UV-Visible spectra in DMSO (λ_{max}/nm); [c] Molar conductance in DMSO ($\Omega^{-1}Cm^2 M^{-1}$);

[d] Magnetic moment (BM); [e] Intrinsic DNA binding constant (M^{-1}); [f] Stern-Volmer Quenching constant.

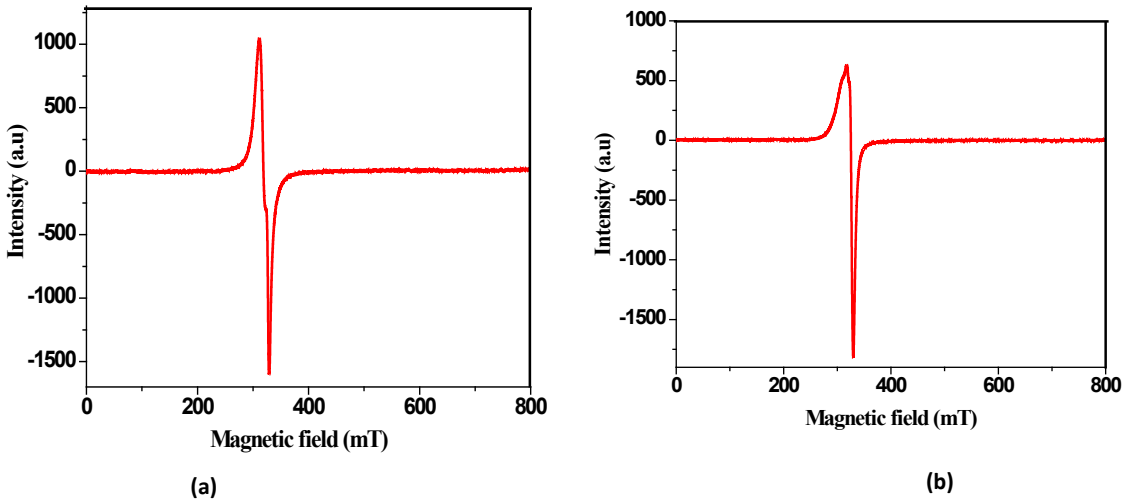

Fig. 3. EPR spectra of complexes **1 (a)** and **2 (b)**

UV-Vis Spectra: In the electronic absorption spectrum of the complex 1, it shows two d–d transitions at 415 nm which can be assigned to $^2B_{1g} \rightarrow {}^2A_{1g}$ transition and 627 nm which can be assigned to $^2B_{1g} \rightarrow {}^2E_g$ transition respectively. It reveals that the complex 1 exists in square planar geometry. Complex 2 shows a d-d band at 649 nm (2) ($^2B_1g \rightarrow {}^2B_2g$ transition) which is consistent with that of square pyramidal geometry around Cu(II). In the UV region, the bands (200-320 nm) were assigned to the intraligand $\pi \rightarrow \pi^*$ transitions.

Magnetic Moment: The magnetic moment for complexes 1 and 2 at room temperature are 1.80 BM suggestive of one unpaired electron system which represents the paramagnetic nature of Cu(II) complexes [38,39].

Epr Spectra: The EPR spectra of complexes 1 and 2 was given in Figure 3 (a &b). According to the data $g\parallel$ and $g\perp$ values for complex 1 is found to be in the range of 2.039–2.061, respectively. From the data, it is clear that $g\perp > 2.0023(ge)$ which suggest the unpaired electron present in d$x2$-$y2$ orbital giving 2B1g as the ground state and the complex is in square planar geometry [40]. The X-band EPR spectra of the complex 2 recorded at room temperature. The complex 2 showing signals according to distorted geometry with values g_{iso}=2.11 for 2, indicates that square-pyramidal geometry [41].

DNA Binding Studies: Since DNA is the primary pharmacological target of many antitumor compounds, the interaction between DNA and metal complexes is of paramount importance in understanding the mechanism. The Cu(II) complexes can bind to the double stranded DNA in different modes on the basis of their structure, charge and type of ligands. Thus, the mode and propensity for binding of the complex to CT-DNA were studied with the aid of following different techniques.

Absorption Spectral Studies: Further evidence for the intercalation of the complexes into the helix was obtained from the UV absorption studies. Monitoring the changes in the absorption spectra of the metal complexes upon addition of increasing amounts of DNA is one of the most widely used methods for determining the overall binding constants. Hypochromism and hyperchromism are the spectral features of DNA concerning its double helix structure. Hypochromism means the DNA binding mode of the complex is intercalation [42,43], which can stabilize the DNA duplex and hyperchromism means the breakage of secondary structure of DNA [44,45]. The UV absorption spectra of complexes 1 (Figure S4; [$]ESI). and 2 in the absence and presence of CT-DNA was given in (Figure 4) Upon addition of increasing amounts of CT-DNA to complexes, hypochromism of the intraligand absorption bands (200-280 nm) of complexes was observed. The observed spectroscopic changes suggest an

intercalative mode of binding that involves a stacking interaction between the aromatic chromophore of the complex and base pairs of DNA [46]. In order to compare the DNA binding affinities of these complexes quantitatively, their intrinsic binding constants (K_b) with CT-DNA were determined (see Eqn 2.[47,48]) and were found to be $1.1x10^4$ M^{-1}, $1.32x10^4$ M^{-1}, for 1 and 2 respectively, indicating their strong binding to DNA. The observed K_b values for 1 and 2 are comparable to that observed for typical classical intercalator, Ethidium bromide (EB-DNA $1.4x10^6$ M^{-1} in 25 mM Tris-HCl/40 mM NaCl buffer (pH =7.9)) [49].

Fluorescence Spectral Studies: The competitive binding experiments with a well established quenching experiment based on the displacement of the intercalating EB from CT-DNA may give further confirmation about the relative binding affinity of the complexes to CT-DNA with respect to EB. EB is a classical intercalator that gives significant fluorescence emission intensity when intercalates into the base pairs of DNA. When it is replaced or excluded from internal hydrophobic circumstance of DNA double helix by other small molecules, its fluorescence emission is effectively quenched by the external polar solvent molecules such as H_2O [50]. The fluorescence quenching curves of EB bound to DNA by complexes 1(Figure S5; [$]ESI) and 2 was given in (Figure 5) As shown in Figure, the EB-DNA system shows characteristic strong emission at ~598 nm when excited at 540 nm, indicating that the intercalated EB molecules have been successfully protected by neighboring DNA base pairs from being quenched by H_2O. A remarkable reduction in emission intensities were achieved as 1 and 2 were added to EB-DNA system, which is a characteristic feature for the intercalative binding of 1 and 2 with DNA [51-53].

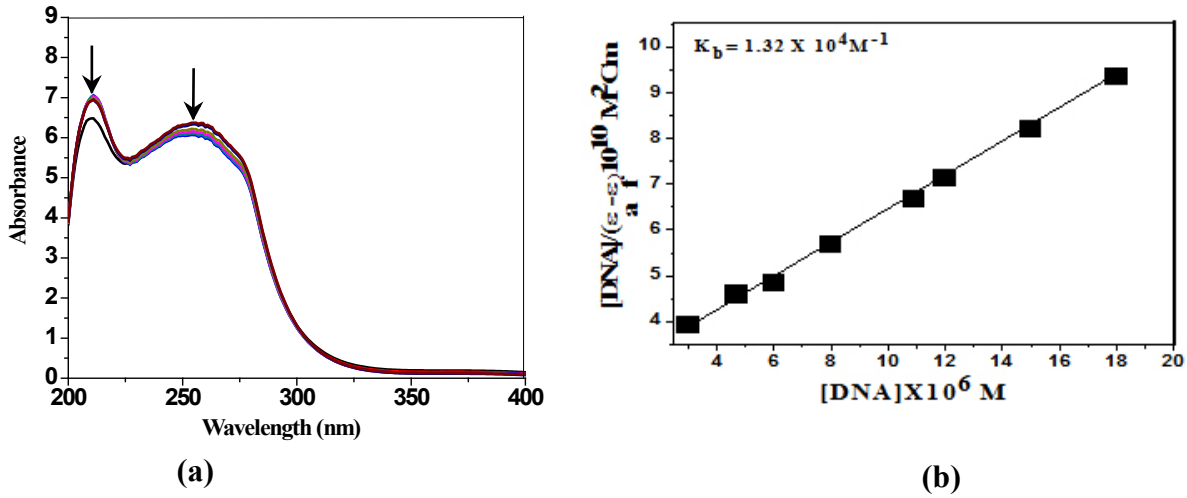

Fig. 4 Absorption spectra of complex **2 (a)** in the absence and presence of increasing amounts of CT-DNA. Conditions: [Complex] = 10µM, [DNA] = 0-10µM. Arrow (¯) shows the absorbance changes upon increasing DNA concentration (**b)** linear plot for the calculation of the intrinsic DNA binding constant, (**K_b**).

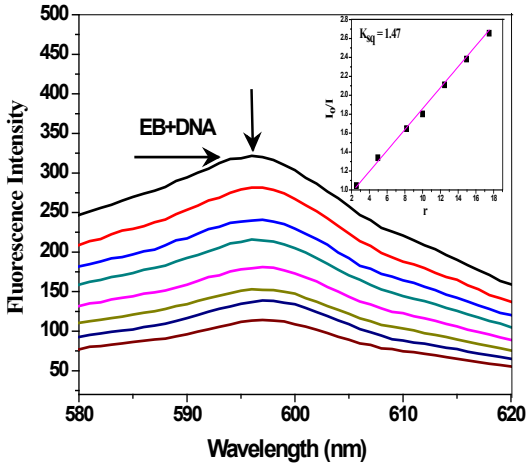

Fig. 5. Emission spectra of EB bound to CT-DNA in the absence and presence of complex **2**

r = [complex] / [DNA]. λ_{ex} = 540 nm, Inset: Stern-Volmer quenching curve

The extent of reduction of emission intensity gives a measure of the binding propensity of the complex to DNA. The quenching efficiency for each complex is evaluated by the Stern-Volmer constant K_{sq}, which varies with the experimental conditions [54]:

$I_o/I = 1+K_{sq}.r$---------- (2)

where I_o and I are the fluorescence intensities in the absence and presence of the complex, respectively, and r is the concentration ratio of the complex to DNA. K_{sq} is a linear Stern-Volmer quenching constant. The quenching plots (insets of respective figures) illustrate that the quenching of EB bound to DNA by the complexes are in good agreement with the linear Stern Volmer equation, which also indicate that the complexes bind to DNA. The K_{sq} value is obtained as the ratio of the slope to intercept. The K_{sq} values for the complexes 1 and 2 are 0.95, 1.47 respectively. Such values of quenching constant suggest that the interaction of complexes with DNA is strong [55, 56].

CD Spectral Studies: CD spectroscopy is one of the most sensitive ways and used to elucidate the changes, the conformational variations of DNA upon interaction with small molecules (often organic ligands or metal complexes) in solution. CD spectrum of CT-DNA exhibits a positive band at 277 nm (base stacking) and a negative band at 248 nm (helicity). The observed CD spectrum of CT DNA consists of a positive band at 274 nm due to base stacking and a negative band at 245nm caused by helicity, which are characteristic of DNA in right-handed B-form. CD spectral variations of CT-DNA in the UV region were recorded by the respective addition of complexes 1(Figure S6; [§]ESI) and 2, as shown in Figure 6, the positive band (~274 nm) decreased significantly in intensity while the negative band (~245 nm) decreased only slightly in intensity with the increase of the complexes, suggesting that complexes induce disturbance on DNA base stacking more than on DNA right-handed helicity and the characteristics of the B form CD spectrum is still conserved and that the arrangement of the DNA bases is somewhat altered. These changes are indicative of an intercalative mode in the binding of these complexes [57].

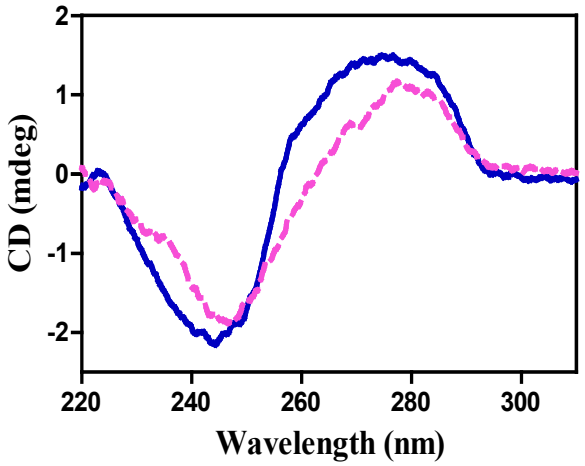

Fig. 6. CD spectra of CT-DNA (100 μM) in the absence (——), in the presence of complex **2**

(----) in 10 mM phosphate buffer solution, [Complex] = 100 μM.

Docking Studies: We used Patch Dock server to understand how these ligand (Figure S7; [§]ESI) and metal complexes interact with DNA. The results were analysed and best solution was selected on the basis of the Patch Dock scores, areas and desolvation energies. The Area (A°) is more it occupy the more space and results high patch dock score (Table 2). Close-up views of the best scored docked complex with DNA are shown in Figure 7(a&b).

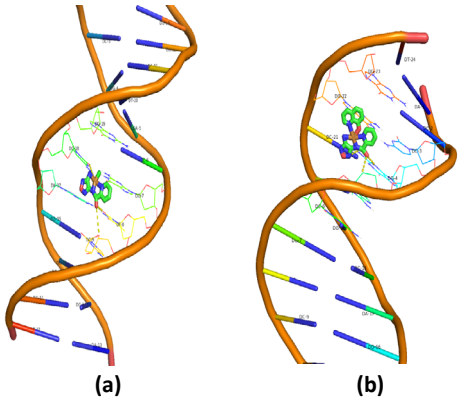

Fig. 7. Molecular Docking of complexes **1** and **2**.

Table 2. Patch Dock score, surface area and desolvation energies of DFPA, complexes **1** and **2**.

Complex	Patch Dock score	Area (Å²)	ACE[a] (kcal/mol)
DFPA ligand	1696	173.6	-278.89
Complex **1**	1798	181.4	-315.07
Complex **2**	2042	218.1	-405.43

a – desolvation energy

It is confirmed by analysing the bond length that the interactions involved occur not only via the hydrogen bonds but also through weak vander wall forces at distances >2.5 Å. The docking data reveal that the complexes 1 and 2 bind to DNA through an intercalative interaction, a preferred mode of interaction for anti-cancer activities [58].

DNA Cleavage : Attempts were also made to cleave DNA through hydrolysis of phosphodiester bond. Since this process does not require any external agents and light it has biological significance. Hydrolytic cleavage experiments were performed by treating supercoiled pUC19 DNA with different concentrations of complexes in the absence of external agents. DNA cleavage was not observed for controls, in which complex was absent (Lane 1). With increasing concentration of complexes 1 and 2 the intensity of Form I of pUC19 DNA diminishes gradually with concomitant increase of nicked form (Form II) shown in Figure 8(a&b) as bar diagrams. Complexes 1 and 2 show concentration dependent relaxation of SC DNA to NC form. For 1 and 2, the chemical nuclease activity follows the order 2>1.

***In Vitro* Cytotoxicity Assay:** The *in vitro* cytotoxic activity of the complexes 1 and 2 were investigated against human cervical carcinoma (HeLa), Human pancreatic carcinoma (MiaPaca-2) and Murine melanoma cells (B16F10) by using the MTT assay for cell viability (Figure 9 (a,b,c)). The results revealed that the concentration dependent decline in the number of viable HeLa cells. The cytotoxicity of complex 1 is comparable with that of Cis-Platin, where as complex 2 exhibits much higher cytotoxicity than Cis-Platin suggesting a promising future drug. The IC_{50} values show that the complex 2 exhibits higher inhibitory effect than Cis-Platin, 8HQ and complex1 against lung cancer cell line (H460), Mouse liver cancer cell line (Hepa 1-6) and Murine melanoma cells (B16F10) (Table 3). The bar diagrams are shown in (Figure S8 [§]ESI).

Confocal Microscopy: The cellular uptake of metal-based anticancer drugs is of importance for its effectiveness against tumors. In order to assess the intracellular localization of complexes inside the human cervical carcinoma (HeLa) cells, confocal microscopic experiments were performed as an initial investigation of its applicability as a fluorescent probe for live-cell applications. The incubation of HeLa cells with the complexes 1 and 2 at 37^0 C under a 5% CO_2 atmosphere resulted in an efficient cellular uptake. To confirm its nuclear localization, the cell was subjected to staining for which the cell treated with complexes 1 and 2 was thoroughly washed, stained with a fluorescent dye, DAPI (4`,6-diamidino-2-phenylindole), a DNA selective fluorescent probe and after fixation, the images were recorded (Figure 10 (a&b)). The relative overlapping fluorescence intensities of compound and DAPI confirm the localization of compound with DNA. Further, the co-localization of complexes 1 and 2 with DAPI, corroborates the interaction of this compound with DNA under live conditions. Hence, the live imaging studies revealed that Cu(II) complex act as a future potential chemotherapeutic agent.

Conclusions

Two new Cu(II) complexes [Cu(II)(DFPA)Cl] (1:1) (1) and [Cu(II)(DFPA)(8HQ)](1:1:1) (2), where DFPA is N-(4-Amino-1,2,5-Oxadiazole-3-yl) Picolinamide derived from the amide linkage of picolinic acid and 3,4-diaminofurazan with HATU reagent, were synthesized and characterized. Complexes 1 and 2 exhibit square planar and square pyramidal geometries. The experimental results suggest that the complexes interact with CT-DNA by an intercalative mode of binding. The gel electrophoresis

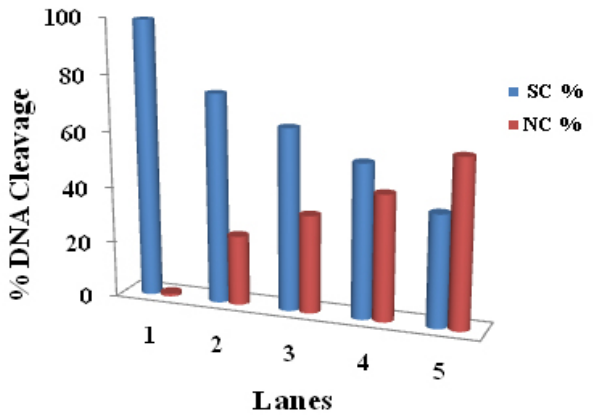

(a) Lane 1, DNA control; Lane 2, DNA+**1** (100 µM); Lane 3, DNA+**1** (200 µM); Lane 4, DNA+**1** (250 µM); Lane 5, DNA+ **1** (300 µM).

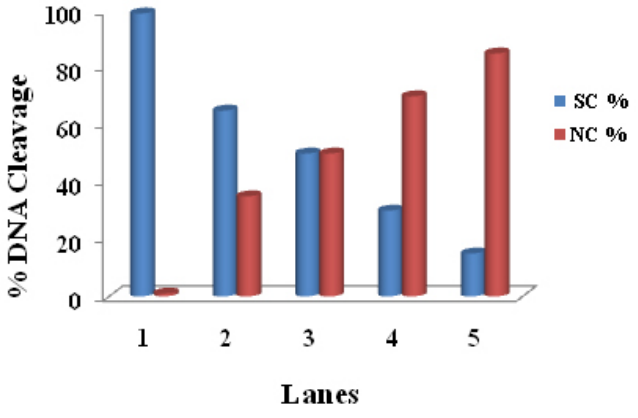

(b) Lane 1, DNA control; Lane 2, DNA+**2** (100 µM); Lane 3, DNA+**2** (200 µM); Lane 4, DNA+**2** (250 µM); Lane 5, DNA+ **2** (300 µM).

Fig. 8. Hydrolytic cleavage of supercoiled pUC19 plasmid DNA at 37°C in 5 mM Tris. HCl / 5 mM NaCl buffer by **1** and **2**.

Table 3. In vitro Cytotoxicity (IC_{50} μM) of complexes 2,Cisplatin and 8HQ after 24 h incubation on HeLa, MiaPaca, B16F10, H460 and Hepa1-6 cell lines.

Cell lines	HeLa	MiaPaca-2	B16F10	H460	Hepa 1-6
[Cu(II)(DFPA)(8HQ)] (2)	5.0±0.6	5.0±0.6	4.8±0.8	5.0±0.8	5.0 ±0.6
Cisplatin	20.0±0.6	18.0 ± 0.5	5.0 ± 0.8	-	-
8HQ	-	-	10.0±0.9	20.0 ± 1.0	10.0 ±0.7

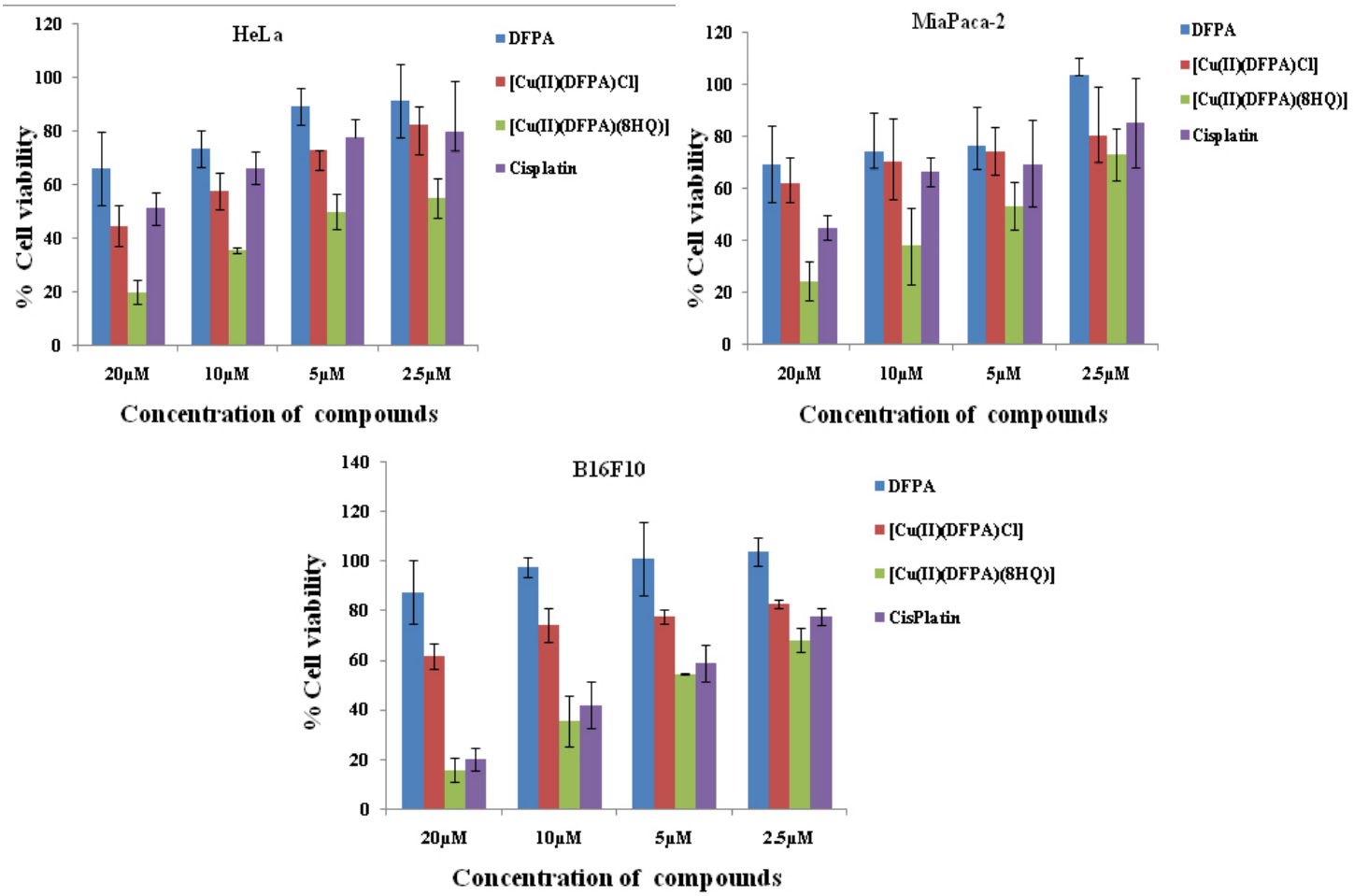

Fig. 9. BAR Diagram showing Cytotoxicity studies of complexes **1** and **2** and Cis platin against the HeLa(**a**), MiaPaca(**b**) and B16F10(**c & d**) cell lines.

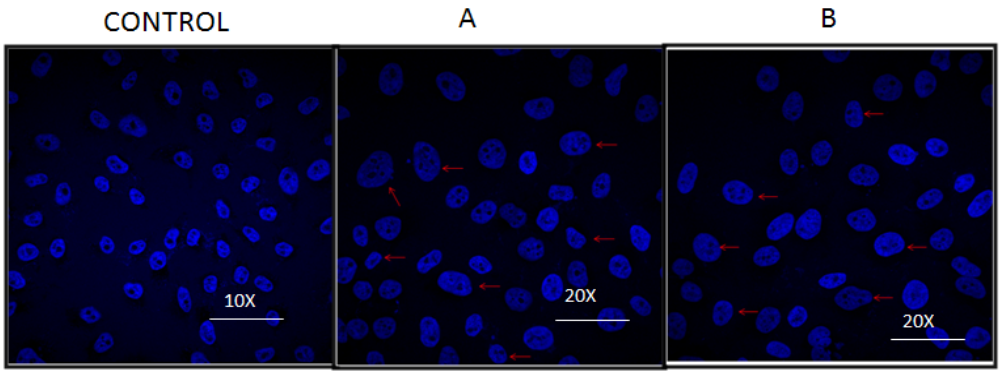

Fig. 10. Nuclear localization studies of complexes **1** and **2 (A** & **B)** in HeLa cells, the treatment concentration is 10 μM, cells were stained with DAPI.

results showed that the complexes 1 and 2 cleave pUC19DNA in a concentration dependent manner and through the hydrolytic pathway. In addition, *in vitro* cytotoxicity of the complexes towards HeLa, MiaPaca-2 and B16F10 cells for cell viability were assayed by the MTT method. Cellular uptake properties on HeLa cell line was studied by confocal microscopy. The IC_{50} values indicate that the complex 2 has better inhibitory effect than Cis-Platin suggesting a future candidate for better anticancer activity.

Acknowledgements

The financial support to PRR from the University Grants Commission (41-286/2012-SR), Govt. of India is gratefully acknowledged.

References

1. Rosenberg B, Vancamp L, Krigas T (1965) Inhibiton of cell division in Escherichia coli by electrolysis products from a platinum electrode. Nature 205: 698-699.
2. Barton K, LolisE (1985) Chiral discrimination in the covalent binding of bis (phenanthroline)dichlororuthenium(II) to B-DNA. J Am Chem Soc 107(3): 708-709.
3. Erkkila KE, Odom DT, Barton JK (1999) Recognition and reaction of metallointercalators with DNA. Chem Rev 99(9): 2777-2796.
4. Charles D, Turner JH, Redmond C (2005) Karyotypicprofiles of Women after clomiphencitrate therapy. BjogIntJObstetGee 80: 264-271.
5. Huppert B (Ed) (1999) Cis-platin, chemistry and Biochemistry of a Heading Anticancer Drug, Wiley VCH, Weinhein.
6. Lippert B (2000) Multiplicity of metal ion binding patterns to nucleobases. Coord Chem Rev 200-202: 487-516.
7. Sigel A, Sigel H (1996) Metal Ions in Biological Systems, Interaction of Metal Ions with Nucleotides, NucleicAcids, and Their Constituents 32 Marcel Dekker New York USA.
8. Marcus Y, Eliezer I (1969) The stability of mixed complexes in solution. Coord Chem Rev 4(3): 273-322.
9. Calvin M, Wilson KW(1945) Stability of chelate compounds. J Am Chem Soc 67(11): 2003-2007.
10. Yang P, Guo M (1999) Interactions of organometallic anticancer agents with nucleotides and DNA. Co.ord Chem Rev 185-186: 189-211.
11. Kakanejadifard A, Azarbani F, Zabardasti A, Kakanejadifard S, Ghasemian M (2013) The synthesis, structural characterization and antibacterial properties of some 2-((4-amino-1,2,5-oxadiazol-3-ylimino)methyl)-4- (phenyldiazenyl)phenol. J Dyes and Pigments 97: 215-221.
12. Cerecetto H, Porcal W(2005) Pharmacological properties of furoxans and benzofuroxans Recent developments. Mini Rev Med Chem 5(1): 57-71.
13. Medana C, Di Stilo A, Visentin S, Fruttero R, Gasco A, et al. (1999) NO donor and biological properties of different benzofuroxans Pharm Res 16(6): 956-960.
14. Buonsanti MF, Bertinaria M, Stilo AD, Cena C, Fruttero R, et al. (2007) Nitric Oxide Donor β2-Agonists: Furoxan Derivatives Containing the Fenoterol Moiety and Related Furazans. J Med Chem 50(20): 5003-5011.
15. Turnbull CM, Cena C, Fruttero R, Gasco A, Rossi AG, et al.(2006) Mechanism of action of novel NO-releasing furoxan derivatives of aspirin in human platelets. J Pharmacol 148(4): 517-526.
16. Cena C, Lolli ML, Lazzarato L, Guaita E, Morini G, et al. (2003) Antiinflammatory, Gastrosparing, and Antiplatelet Properties of New NO-Donor Esters of Aspirin. J Med Chem 46(5): 747-754.
17. Beebe X, Nilius AM, Merta PJ, Soni NB, Bui MH, et al.(2003) Synthesis and SAR evaluation of oxadiazolopyrazines as selective Haemophilus influenzae antibacterial agents. Bioorg Med Chem Lett 13(19): 3133-3136.
18. LoGrasso PV, Feng Y (2009) Rho kinase (ROCK) inhibitors and their application to inflammatory disorders Curr Top. Med Chem 9(8): 704-723.
19. Visentin S, Rolando B, Di Stilo A, Fruttero R, Novara M, et al. (2004) New 1,4-Dihydropyridines Endowed with NO-Donor and Calcium Channel Agonist Properties. J Med Chem 47(10): 2688-2693.
20. Lolli ML, Cena C, Medana C, Lazzarato L, Morini G, et al. (2001) A new class of ibuprofen derivatives with reduced gastrotoxicity. Med Chem 44(21): 3463-3468.
21. Sorba G, Gasco A, Orsetti M (1989) Potential histamine H2-receptor antagonists twin compounds containing diaminofurazan substructure. Arch Pharm 322(9): 579-580.
22. Fernández E, García-Ochoa S, Huss S, Mallo A, Bueno JM, et al. (2002) Solid-phase versus solution synthesis of asymmetrically disubstituted furazano[3,4-b]pyrazines. Tetrahedron Lett 43(27): 4741-4745.
23. Wen-Shan L, Shivaji VM , Chie-Hong W, Ya Ching J, Ching-Fa Y, et al. (2010) Synthesis and structure-activity relationships of novel furazan-3,4-diamide analogs as potent anti-cancer agents. Bioorg Med Chem Lett 20(3): 1148-1152.
24. Grant RS, Coggan SE, Smythe GA (2009) The physiological action of picolinic acid in the human brain. International J Try Res 271-279.
25. Dazzi C, Candiano G, Massazza S, Ponzetto A, Varesio L, et al. (2001) New highperformance liquid chromatographic method for the detection of picolinicacid in biological fluids. J Chromatogr 751(1): 61-68.
26. Smythe GA, Braga O, Brew BJ, Grant RS, Guillemin GJ, et al. (2002) Concurrent Quantification of Quinolinic, Picolinic, And Nicotinic Acids Using Electron-Capture Negative-Ion Gas Chromatography Mass Spectrometry. Anal Biochem 301(1): 21-26.
27. Rebello T, Lonnerdal B, Hurley LS (1982) Picolinic acid in milk, pancreaticJuice, and intestine: inadequate for role in zinc absorption. Am J ClinNutr 35(1): 1-5.
28. Frumento G, Rotondo R, Tenetti M, Domonte G, Benatti U, et al. (2002) Tryptophan- derived catabolites are responsible for inhibition of T and natural killer cell proliferation induced by indoleamine 2,3-dioxygenase J ExperMed 196(4): 459-468.

29. Nordenberg J, Novogrodsky A, Beery E, Patia M, Wasserman L, et al. (1990) Anti-proliferative effects and phenotypic alterations induced by 8-hydroxyquinoline in melanoma cell lines. Eur J Cancer Clin Oncol 26(8): 905-907.

30. Core V, Renaud S, Cannie I, Julienne K, Gouin SG, et al. (2014) Synthesis and Biological Properties of Quilamines II, New Iron Chelators with Antiproliferative Activities. Bioconjug. Chem 25(2): 320-334.

31. Figgi's BN, Lewis J (1967) Modern Coordination Chemistry, Ed. J. Lewis, R.C.Wilkinson, Wiley interscience New York.

32. Marmur JA (1961) procedure for the isolation of deoxyribonucleic acid from micro-organisms. J Mol Biol 3(2): 208-218.

33. Reichmann ME, Rice SA, Thomos CA, Doty P (1954) A further examination of the molecular weight and size of deoxypentose nucleic acid. J. Am. Chem Soc 76(11): 3047-3053.

34. Garland F, Graves DE , Yielding LW, Cheung HC (1980) Comparative studies of the binding of ethidium bromide and its photoreactive analogues to nucleic acids by fluorescence and kinetics, Biochemistry 19(14): 3221-3226.

35. Schneidman-Duhovny D, Inbar Y, Nussinov R, Wolfson HJ (2005) servers for rigid and symmetric docking. Nucl Acids Res 33: 363-367.

36. Duhovny D R, Nussinov H J, Wolfson (2002) Efficient Unbound Docking of Rigid Molecules. In Gusfield et al., Ed. Proceedings of the 2'nd Workshop on Algorithms in Bioinformatics(WABI) Rome, Italy Lecture Notes in Computer Science, Springer Verlag 18: 2452.

37. Nakamoto K (1978) Infrared and Raman Spectra of Inorganic and Coordination compounds, third edition, edited by K.Nakamoto. New York: John Wiley & sons.

38. Basudev M, Sudarshan G, Goswami TK, Anjali AK, Chakravarty AK (2011) Impact of metal on the DNA photocleavage activity and cytotoxicity of ferrocenyl terpyridine 3d metal complexes. Dalton Trans 40(44): 11904.

39. Pathan AH , Bakale RP, Naik GN, Frampton CS, Gudasi KB (2012) Synthesis, crystal structure, redox behavior and comprehensive studies on DNA binding and cleavage properties of transition metal complexes of a fluoro substituted thiosemicarbazone derived from ethyl pyruvate. Polyhedron 34(1): 149-156.

40. Kivelson D, Neiman R (1961) ESR line shapes in glasses of copper complexes. The Journal of ChemicalPhysics 35(1): 149-155.

41. Garcia-Raso A, Juan JF, Adrover B, Moreno V, Mata I (2003) Synthesis, structure and nuclease properties of several ternary Cu(II) peptide complexes with 1,10-phenanthroline. J Inorg Biochem 95(2-3): 77-86.

42. Kelly J M, Tossi A B, McConnell D J, OhUigin C (1985) A study of the interactions of some polypyridylruthenium (II) complexes with DNA using fluorescence spectroscopy, topoisomerisation and thermal denaturation. Nucleic Acids Res 13(17): 6017-6034.

43. Peng B, Chao H, Sun B, Li H, Gao F, Ji LN (2006) DNA interactions of a functionalized ruthenium(II) mixed-polypyridyl complex [Ru(bpy)2p-pd]2+. J Inorg Biochem100(9): 1487-1494.

44. Uma V, Kanthimathi M, Weyhermuller T, Nair BU (2005) Oxidative DNA cleavage mediated by a new copper (II) terpyridine complex: Crystal structure and DNA binding studies. J Inorg Biochem 99(12): 2299-2307.

45. Kumar CV, Asuncion EH (1993) DNA binding studies and site selective fluorescence sensitization of an anthryl probe. J. Am. Chem. Soc 115(19): 8547-8553.

46. WolfA A, Shimer GH, Meehan T (1987) Polycyclic aromatic hydrocarbons physically intercalate into duplex regions of denatured DNA. Biochemistry 26(20): 6392-6396.

47. Mathur S, Tabassum S (2008) Template synthesis of novel carboxamide dinuclear copper(II) complex: spectral characterization and reactivity towards calf-thymus DNA. Biometals 21(3): 299-310.

48. Kumar C V, Barton J K, Turro N L (1985) Photophysics of Ruthenium complexes bound to Double helical DNA. J Am Chem Soc 107(19): 5518-5523.

49. Ma YZ, Yin HJ, Wang KZ (2009) A beta-D-allopyranoside-grafted Ru(II) complex: synthesis and acid-base and DNA-binding properties. J Phys Chem B 113(31): 11039-11047.

50. Lu YY, Gao LH, Han M J, Wang K Z, et al. (2006) DNA Interaction and Antitumor Activities of Ruthenium(II) Polypyridyl Complex Eur J. Inorg. Chem 430-436.

51. Wu LM , H.B Teng , Ke XB, Xu WJ, Su JT, et al. (2007) Copper(II) complexes of salicylaldehyde hydrazones: synthesis, structure, and DNA interaction. Chem Biodiver 4(9): 2198-2209.

52. Lakowicz JR, Webber G (1973) Quenching of protein fluorescence by oxygen. Detection of structural fluctuations in proteins on the nanosecond time scale. Biochemistry 12(21): 4171-4179.

53. Baguley BC, Bret ML (1984) Quenching of DNA-ethidium fluorescence by amsacrine and other antitumor agents: a possible electron-transfer effect. Biochemistry 23(5): 937-943.

54. Liu J, Zhang TX, Lu TB, Qu LH, Zhou H, et al. (2002) DNA-binding and cleavage studies of macrocyclic copper(II) complexes. J Inorg. Biochem 91(1): 269-276.

55. Selvi P T, Palaniandavar M (2002) Spectral, viscometric and electrochemical studies on mixed ligand cobalt(III) complexes of certain diimine ligands bound to calf thymus DNA Inorg. Chim. Acta 337: 420-428.

56. Zhang Z , Qian XH, Yang Y, Liu F (2006) Study on the interaction between 4-(2-diethylamino-ethylamino)-8-oxo-8H-acenaphtho[1,2-b] pyrrole-9-carbonitrile and DNA by molecular spectra. Int. J. Biol. Macromol 38(1): 59-64.

57. Wu BY, Gao LH, Duan ZM, Wang KZ (2005) Syntheses and DNA-binding studies of two ruthenium(II) complexes containing one ancillary ligand of bpy or phen [Ru(bpy)(pp[2,3]p)2](ClO_4)2 and [Ru(phen)(pp[2,3]p)2](ClO_4)2. J. Inorg. Biochem 99(8): 1685-1691.

58. Pulimamidi RR, Ravula C, Battu S (2016) New bio-based cu(II) complexes and study of their anti-cancer activities. J Fluoresc 26(4): 1183-1197.